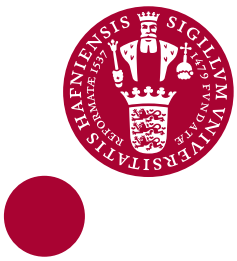

Temperature and fluid velocity on the freeze-out surface from pi, K, and p spectra in pp, p-Pb, and Pb-Pb collisions

Mazeliauskas, Aleksas; Vislavicius, Vytautas

Published in:
Physical Review C

DOI:
10.1103/PhysRevC.101.014910

Publication date:
2020

Document version
Publisher's PDF, also known as Version of record

Temperature and fluid velocity on the freeze-out surface from π, K, and p spectra in pp, p-Pb, and Pb-Pb collisions

Aleksas Mazeliauskas[*]
Theoretical Physics Department, CERN, CH-1211 Genève 23, Switzerland
and Institut für Theoretische Physik, Universität Heidelberg, Philosophenweg 16, D-69120 Heidelberg, Germany

Vytautas Vislavicius[†]
Niels Bohr Institutet, Københavns Universitet, Blegdamsvej 17, DK-2100 Copenhagen, Denmark

(Received 12 September 2019; published 17 January 2020)

We present a new approach to take into account resonance decays in the blast-wave model fits of identified hadron spectra. Thanks to precalculated decayed particle spectra, we are able to extract, in a matter of seconds, the multiplicity dependence of the single freeze-out temperature $T_{\rm fo}$, average fluid velocity $\langle\beta_{\rm T}\rangle$, velocity exponent n, and the volume dV/dy of an expanding fireball. In contrast to blast-wave fits without resonance feed-down, our approach results in a freeze-out temperature of $T_{\rm fo} \approx 150$ MeV, which has only weak dependence on multiplicity and collision system. Finally, we discuss separate chemical and kinetic freeze-outs separated by partial chemical equilibrium.

DOI: 10.1103/PhysRevC.101.014910

I. INTRODUCTION

The relativistic hadron collisions explore the properties of dense nuclear matter at temperatures several times higher than that of the pseudocritical QCD temperature $T_c = 156.5 \pm 1.5$ MeV [1], i.e., the state of deconfined quarks and gluons. Remarkably, the study of produced hadron and light nuclei abundances indicates an apparent thermal particle production at constant chemical freeze-out temperature $T_{\rm chem} \approx T_c$, as shown by fits of the statistical hadronization model (SHM) [2]. Furthermore, phenomenological models based on viscous fluid description of the quark-gluon plasma (QGP) expansion successfully reproduce many soft hadronic observables [3–7]. Global fits to experimental data can then be used to extract the model parameters and the transport properties of dense QCD matter [8].

One of the earliest and simplest models of hadron production from a flowing medium is the blast-wave model [9]. It is based on calculating particle emission from a parametrized freeze-out surface of temperature $T_{\rm fo}$ and radial velocity profile $\beta_T(r)$. The primary particle spectra are taken to be thermal in the local rest frame of the fluid. Then the experimentally observed hadrons, e.g., pions, kaons, or protons, are calculated by adding the decay feed-down from the short-lived primary resonances to the initial thermal abundances. In general, freeze-out with only direct decays gives a reasonably good description of the data [10–12], but neglects possible rescattering and regeneration of hadrons, which can be modelled by hadronic after-burners [13,14]. The blast-wave model can be simplified even further by using thermal spectra of pions, kaons, and protons to directly fit the measured particle spectra. As decay feed-down significantly modifies the magnitude and momentum dependence of distributions, individual normalizations are introduced for each particle species and the momentum range for the fit is restricted [15]. In this case the extracted freeze-out temperature and radial velocity profiles are interpreted as temperature and velocity at the kinetic particle freeze-out. This is the routine analysis procedure performed for measured identified particle spectra as a convenient way to characterize and compare the soft particle production at different centralities and collision systems [15–19].

In this paper we present a procedure for the blast-wave model fits, which includes the feed-down from resonance decays. We are certainly not the first to include resonance decays in the blast-wave model, as it was done already in [9] and other studies [10,20–22]. However, up to now the generation of primary thermal hadrons and their decays were two separate steps, the latter computed by either Monte Carlo generators [23–26], or semianalytic treatments of decay integrals [27,28]. This amounts to considerable computational costs, as for each set of model parameters a large number of primary hadron spectra need to be generated and then decayed through thousands of decay channels [29]. Instead we use a recently published method of efficient calculation of direct resonance decays [30,31]. The technique is based on first calculating the resonance decays in the fluid rest frame

[*]aleksas.mazeliauskas@cern.ch
[†]vytautas.vislavicius@cern.ch

and only then finding the final particle spectra for a fluid cell moving with some velocity $u^\mu(x)$. In this approach the primary resonances and decays need to be evaluated only once for a given temperature and chemical potential, which greatly simplifies and speeds up the fitting procedure.

II. BLAST-WAVE FIT WITH RESONANCE DECAY FEED-DOWN

In a boost invariant blast-wave freeze-out model, particles are produced from a constant time $\tau_{\rm fo}$ and temperature $T_{\rm fo}$ freeze-out surface with transverse radius R and a powerlike velocity profile [9],

$$\beta_T \equiv \frac{u^r}{u^\tau} = \beta_{\rm max}\left(\frac{r}{R}\right)^n. \tag{1}$$

Thermal particle production from a fluid cell of temperature $T_{\rm fo}$ moving with a four-velocity u^μ can be calculated according to the Cooper-Frye formula [32],

$$E_{\mathbf{p}}\frac{dN}{d^3\mathbf{p}} = \frac{\nu}{(2\pi)^3}\int_\sigma f(-u^\nu p_\nu, T_{\rm fo}, \mu)p^\mu d\sigma_\mu. \tag{2}$$

Here $\nu = (2S+1)$ is the spin degeneracy, $d\sigma_\mu$ is the freeze-out surface element (for blast-wave surface $d\sigma_\mu = (\tau_{\rm fo} d\eta r d\phi dr, 0, 0, 0)$, μ is the chemical potential, $\bar{E}_p = -u^\nu p_\nu$ is the fluid-frame energy of the particle, and f is the thermal particle distribution function.

The unstable resonances produced on the freeze-out surface according to Eq. (2) decay and nontrivially modify the momentum spectra of long-lived hadrons. It was shown in Ref. [30] that decay feed-down modification for thermally produced hadrons can be captured by two scalar distribution functions, $f_1^{\rm eq}$ and $f_2^{\rm eq}$,[1] which generalize the Cooper-Frye freeze-out integral to

$$E_{\mathbf{p}}\frac{dN}{d^3\mathbf{p}} = \frac{\nu}{(2\pi)^3}\int_\sigma \left[f_1^{\rm eq}(p^\mu - \bar{E}_{\mathbf{p}}u^\mu) + f_2^{\rm eq}\bar{E}_{\mathbf{p}}u^\mu\right]d\sigma_\mu. \tag{3}$$

Given a list of resonances and decay channels functions $f^{\rm eq}_{i=1,2}(-u^\nu p_\nu, T_{\rm fo}, \mu)$ can be easily computed using publicly available code [31]. For the azimuthally symmetric and boost-invariant blast-wave surface the decayed particle spectra simplifies to a one-dimensional integral [30]

$$\frac{dN}{2\pi p_T dp_T dy} = \frac{\nu}{(2\pi)^3}\int_0^R dr\ \tau_{\rm fo} r\, K_1^{\rm eq}(p_T, \beta_T(r)). \tag{4}$$

The freeze-out kernel $K_1^{\rm eq}(p_T, \beta_T, T_{\rm fo}, \mu)$ can be evaluated in advance for a range of values (p_T, β_T) by azimuthal and space-time rapidity integrals of functions $f^{\rm eq}_{i=1,2}$,

$$K_1^{\rm eq}(p_T, \beta_T) = \int_0^{2\pi} d\phi \int_{-\infty}^{\infty} d\eta \left\{f_1^{\rm eq}(\bar{E}_{\mathbf{p}})m_T\cosh(\eta) + \left[f_2^{\rm eq}(\bar{E}_{\mathbf{p}}) - f_1^{\rm eq}(\bar{E}_{\mathbf{p}})\right]\bar{E}_{\mathbf{p}}u^\tau\right\}, \tag{5}$$

where $\bar{E}_{\mathbf{p}} = m_T u^\tau \cosh(\eta) - p_T u^r \cos\phi$ is the particle energy in the fluid rest frame, the transverse mass is defined as $m_T = \sqrt{p_T^2 + m^2}$, and radial velocity is $u^r = \beta_T/\sqrt{1-\beta_T^2}$. Equation (4) should be compared with the analogous equation in the standard blast-wave fit, where the thermal freeze-out kernel is given by the corresponding integral of the Boltzmann distribution [9],

$$K_1^{\rm th}(p_T, \beta_T) = 4\pi m_T \mathcal{I}_0\left(\frac{p_T u^r}{T_{\rm fo}}\right)\mathcal{K}_1\left(\frac{m_T u^\tau}{T_{\rm fo}}\right). \tag{6}$$

The crucial difference is that our freeze-out kernel $K_1^{\rm eq}(p_T, \beta_T)$ already contains the feed-down contributions from the unstable resonances. Therefore different particles produced from the same freeze-out surface have the same normalization in Eq. (4), namely the freeze-out volume per rapidity $dV/dy = \tau_{\rm fo}\pi R^2$ (in the laboratory frame).

Finally we note that although in Eq. (4) we considered a very specific freeze-out surface, the procedure can be straightforwardly extended to more complicated freeze-out surfaces by introducing additional freeze-out kernels [30].

III. PARTIAL CHEMICAL EQUILIBRIUM

To allow for separate chemical and kinetic freeze-outs we employ the partial chemical equilibrium (PCE) model [33,34]. In this model the quasistable hadrons b maintain an approximate kinetic equilibrium through elastic scatterings, but the particle ratios are fixed at the chemical freeze-out temperature $T_{\rm chem}$. Then at the kinetic freeze-out the distribution function of resonance a is given by a thermal distribution at temperature $T_{\rm fo} = T_{\rm kin}$, but with chemical potential $\tilde{\mu}_a(\mu_b) = \sum_b N_{a\to b}\mu_b$, where $N_{a\to b}$ is the number of decay products b, and μ_b is the chemical potential of the quasistable species b. Assuming ideal hydrodynamic evolution between the chemical and kinetic freeze-outs, chemical potentials μ_b are such that entropy per quasistable particle b is conserved, i.e., we need to solve the implicit equation for μ_b,

$$\frac{\sum_a N_{a\to b} n_a(T_{\rm chem}, 0)}{\sum_a s_a(T_{\rm chem}, 0)} = \frac{\sum_a N_{a\to b} n_a(T_{\rm kin}, \tilde{\mu}_a(\mu_b))}{\sum_a s_a(T_{\rm kin}, \tilde{\mu}_a(\mu_b))}, \tag{7}$$

where the sum goes over all resonance species a and n_a, s_a are the number and entropy density for an ideal gas of resonance species a. Then the freeze-out kernel for partial chemical equilibrium

$$K_1^{\rm eq}(p_T, \beta_T; T_{\rm kin}, \mu(T_{\rm kin}, T_{\rm chem})) \tag{8}$$

can be computed by decaying hadrons at the kinetic freeze-out $(T_{\rm kin}, \tilde{\mu}_a(\mu_b))$ using the same techniques [30].

IV. SETUP

We evaluated the irreducible scalar distributions $f^{\rm eq}_{1,2}$ for π, K, p, Λ, Ξ, and Ω using the publicly available code `FastReso` [31]. We use a recent list of resonances and decay channels (including less established states) [35–37] derived from 2016 edition of Particle Data Group book [38]. In total, we perform 3291 two-body and 513 three-body strong and electromagnetic decays for 739 resonances with masses up to 3.0 GeV/c^2. For the single freeze-out fits of π, K, p spectra, we evaluated the freeze-out kernels $K_1^{\rm eq}$ for temperatures in a 130–180-MeV interval in 0.5-MeV steps and kept the baryon

[1] $f^{\rm eq}_{i=1,2}$ are components of irreducible decomposition under rotations of the decayed particle spectra in the fluid rest frame [30].

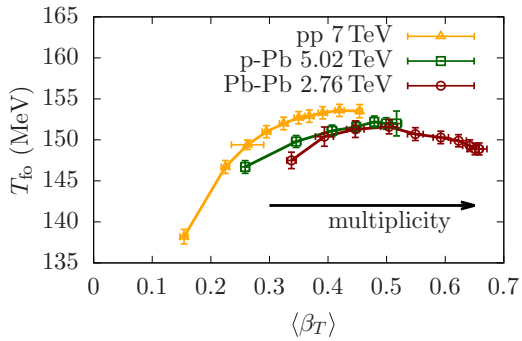

FIG. 1. Blast-wave freeze-out temperature T_{fo} versus mean transverse velocity $\langle\beta_T\rangle$ in pp, p-Pb, and Pb-Pb collisions including the feed-down of resonance decays. Spectra of π, K, and p are fitted in $0.5 < p_T < 3.0$ (GeV/c) momentum range. Error bars correspond to fit parameter uncertainties.

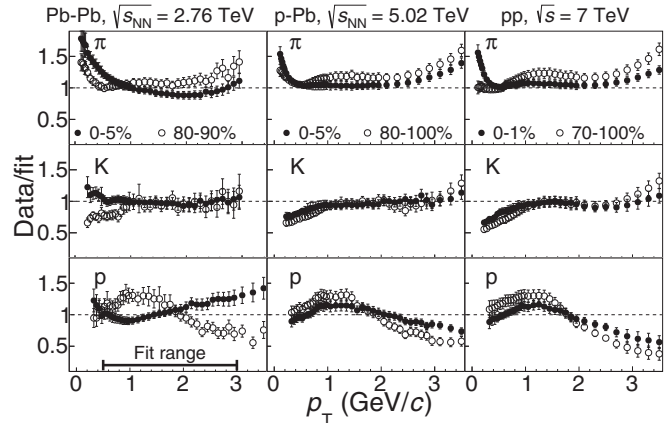

FIG. 2. Transverse momentum spectra of π, K, p divided by the blast-wave fit with resonance decays at most central (full symbols) and peripheral (open symbols) centrality classes. Error bars correspond to statistical and systematic uncertainties of the data summed in quadrature.

chemical potential $\mu_B = 0$. For calculating PCE freeze-out kernels, Eq. (8), we followed Ref. [39] and conserved the particle number of π, K, η, ω, p, n, η', ϕ, Λ, Σ, Ξ, $\Lambda(1520)$, $\Xi(1530)$, and Ω hadrons. Then we fixed the chemical freeze-out temperature and varied T_{kin} in 1-MeV steps in a 100–200-MeV interval.

V. RESULTS

The data considered in this work has been published by the ALICE Collaboration [40] and includes π, K, and p spectra measured as a function of centrality and multiplicity in pp collisions at $\sqrt{s} = 7$ TeV [41], p-Pb collisions at $\sqrt{s_{NN}} = 5.02$ TeV [42], and Pb-Pb collisions at $\sqrt{s_{NN}} = 2.76$ TeV [15]. The blast-wave model parameters are extracted by simultaneously fitting the π, K, p spectra in the transverse momentum range $0.5 < p_T < 3.0$ (GeV/c), where each data point is considered with a weight given by the statistical and systematic uncertainties summed in quadrature. We checked that extracted parameters are insensitive to the choice of momentum range for central and midcentral Pb-Pb collisions and p-Pb and pp results show only modest dependence on the fit ranges (see Appendix). We find a very good fit for Pb-Pb spectra with χ^2/dof in the range 0.5–2.9. For smaller collision systems χ^2/dof grows from 1.5 in the highest multiplicity p-Pb collisions to 8.2 in the lowest multiplicity pp bin. For completeness the tables of the best fit values, their uncertainties, and χ^2/dof are given in Appendix.

In Fig. 1 we show the extracted freeze-out temperature T_{fo} plotted as a function of mean radial velocity $\langle\beta_T\rangle \equiv 2\beta_{max}/(2+n)$ and collision system. All systems show stronger radial flow with increasing multiplicity, but only modest temperature dependence. We see that for Pb-Pb collisions the freeze-out temperature is in the 148–152-MeV range[2] and close to the chemical freeze-out temperature $T_{chem} = 156.5 \pm 1.5$ MeV obtained by the statistical model fitted to light and multistrange hadrons in the most central collisions [2]. Studies of centrality dependence of thermal model parameters also find weak temperature dependence, but the temperature is higher than extracted in out fits [43–45]. We note that in our model we use only π, K, p spectra and do not introduce baryon chemical potential, canonical suppression, or strangeness undersaturation effects. In smaller systems we observe similar values of freeze-out temperature, and in the case of p-Pb collisions we find overlapping freeze-out temperature and radial flow values compared to Pb-Pb. Finally, pp collisions tend to have smaller average radial flow, but the temperature dependence is comparable to other systems, except for the lowest multiplicity bin.

Our results in Fig. 1 are noticeably different from the usual blast-wave fits without resonance decays, which show strong freeze-out temperature dependence on centrality in Pb-Pb collisions [15]. To understand this difference, we repeated the fits for Pb-Pb data by allowing independent normalizations of each particle spectrum. We found that χ^2/dof of such a fit does not have a well localized minimum in the freeze-out temperature T_{fo}, but instead has a very shallow region over the entire considered range of temperature. In fact, it was already shown in Ref. [9], that due to the feed-down of heavier resonances, pions respond to radial flow much like heavy particles and equally good fits to particle spectra can be obtained for different values of freeze-out temperature. In contrast, the blast-wave fit without resonance decays erroneously singles out a particular combination of temperature and radial flow.

Next we study the ratios of measured hadron spectra to the improved blast-wave model fits, which are shown in Fig. 2 for different collision systems and most central and most peripheral centrality bins. We find that π, K, and p spectra are described by the model within the ≈2–4σ range for momenta $0.5 < p_T < 3.0$ (GeV/c), suggesting that the primary hadrons are emitted from a fluid expanding with common velocity field. The ratios are flat for pions and kaons, but the proton spectra-to-fit ratio shows a residual evolution with p_T, which can be attributed to the rescatterings in the hadronic gas

[2]We note that including additional resonances states from PDG2016+ systematically lowers the extracted freeze-out temperature, but the radial flow remains unchanged.

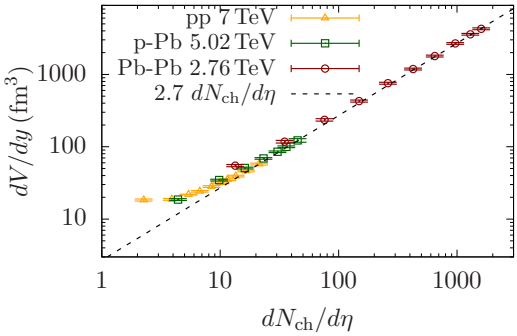

FIG. 3. Extracted freeze-out volume per rapidity dV/dy (in the laboratory frame) as a function of multiplicity for different collision systems. Error bars correspond to fit parameter uncertainties.

phase, which generally boost heavier particles towards higher momenta [12].

We would like to emphasize that including resonance decays in the blast-wave fits allows us to use a single normalization factor for all particle species. The extracted factor can be interpreted as the freeze-out volume per unit rapidity of the fireball and is proportional to the overall multiplicity $dN_{ch}/d\eta$, as shown in Fig. 3. Because of fixed normalization, the extracted blast-wave model parameters β_{max}, T_{fo}, n, and dV/dy from fits to π, K, and p spectra can be used to predict heavier hadrons, such as Λ, Ξ, Ω [18,19,46–48]. We show the data to model ratios in Fig. 4 (π, K, p spectra were refitted in the same centrality bins). The model predictions for Ξ and Ω are good and only Λ spectra is somewhat underpredicted (similar discrepancies are also seen in full hydrodynamic simulations [12]).

Finally, we consider the blast-wave fits with distinct chemical and kinetic freeze-outs using partial chemical equilibrium model. We fix the chemical freeze-out temperature T_{chem} (and

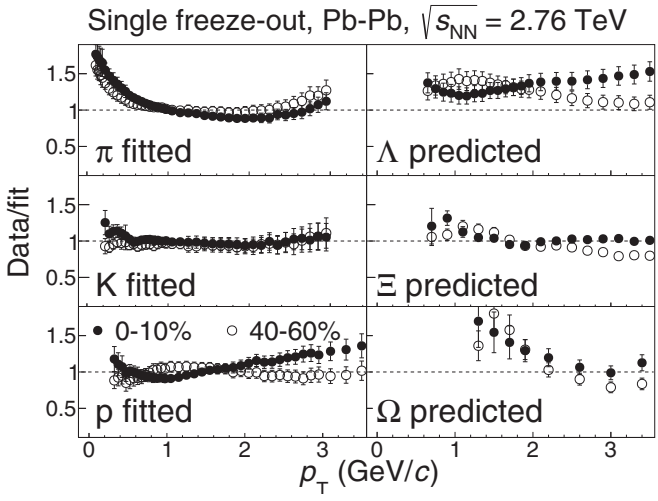

FIG. 4. Left: Data to fit ratios of π, K, p spectra in single freeze-out blast-wave model. Right: Data to prediction ratios of Λ, Ξ, Ω spectra obtained using the same blast-wave fit parameters. Error bars correspond to statistical and systematic uncertainties of the data summed in quadrature.

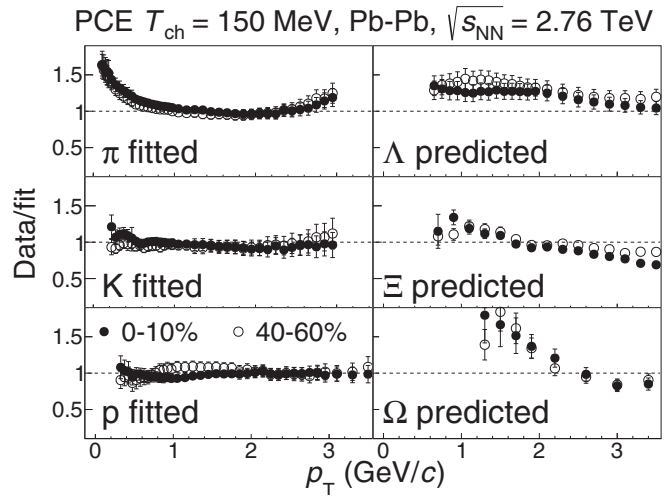

FIG. 5. Left: Data to fit ratios of π, K, p spectra in partial chemical equilibrium model with chemical freeze-out at $T_{chem} = 150$ MeV. Right: Data to prediction ratios of Λ, Ξ, Ω obtained using the same blast-wave fit parameters. Error bars correspond to statistical and systematic uncertainties of the data summed in quadrature.

hence particle ratios) and vary the kinetic freeze-out temperature T_{kin}. In Fig. 5. we show the spectral ratios for Pb-Pb collisions at two different centralities for $T_{chem} = 150$ MeV. The data to model ratio for protons becomes flat in 0–10% centrality with the kinetic freeze-out temperature $T_{kin} = 126 \pm 2$ MeV, while for 40–60% centrality the kinetic and chemical freeze-out temperatures become approximately equal. For pp and p-Pb collisions, we do not obtain a convergent fit, with $T_{kin} > T_{chem}$ reaching the upper limit (200 MeV) of the fitting range. This points out to the fact that additional observables, e.g., short-lived resonances, are needed to differentiate chemical and kinetic freeze-outs [49].

VI. CONCLUSIONS AND OUTLOOK

We performed the multiplicity and collision system analysis of identified hadron spectra using the blast-wave model with resonance decays for pp, p-Pb, and Pb-Pb collisions at the LHC. Thanks to the inclusion of decay feed-down, we were able to fit π, K, p spectra in a wide momentum range $0.5 < p_T < 3.0$ (GeV/c) and extract the common freeze-out volume, freeze-out temperature, and the radial flow parameters. In contrast to traditional blast-wave fits, our fits take into account both the shape and relative normalization of particle spectra. Consequently, our method produces a single freeze-out temperature, which is relatively insensitive to the multiplicity, system size, or fitting ranges. By using independent normalization of spectra we checked that with decay feed-down, only the shape of pion, kaon, and proton spectra alone is not sufficient to unambiguously determine the freeze-out temperature and radial flow [9]. Our fit of π, K, p spectra is in $\approx$2–4σ agreement with experimental data in the fitting range $0.5 < p_T < 3.0$ (GeV/c) for all multiplicity classes and collision systems. Furthermore, using the extracted freeze-out volume we were able to predict multistrange particle spectra (Λ, Ξ, Ω) without additional model parameters.

Finally, introducing separate kinetic and chemical freeze-outs separated by partial chemical equilibrium phase slightly improved the fit of proton spectra in central 0–10% Pb-Pb collisions with $T_{\rm kin} \approx 126 \pm 2$ MeV, which grows towards and past $T_{\rm chem}$ in more peripheral collisions. However the procedure does not result in physical parameter values in small multiplicity collisions. We conclude that particle spectra beyond the long lived π, K, p are needed to constrain the kinetic freeze-out temperature.

The most significant aspect of our study is the practical demonstration that simple data analysis including the important effect of decay feed-down can be done in a computationally efficient way. By first calculating the decayed particle spectra in the fluid frame for a range of freeze-out parameters [30,31], we were able to perform the blast-wave fit analysis of particle spectra in a matter of seconds. This practical approach opens up a way for simple but realistic studies of particle production in hadronic collisions using parametrized freeze-out surfaces. Useful physical insight could be gained by studying the shape of freeze-out surface in small collision systems [50], the effect of viscous corrections to particle spectra and elliptic flow [12,51–53], the freeze-out criteria [54,55], and inclusion of additional observables [56–60]. These studies would clearly complement the ongoing multiparameter hydrodynamic modeling of heavy-ion collisions, which ultimately can be used to determine the properties of the QGP [8,61].

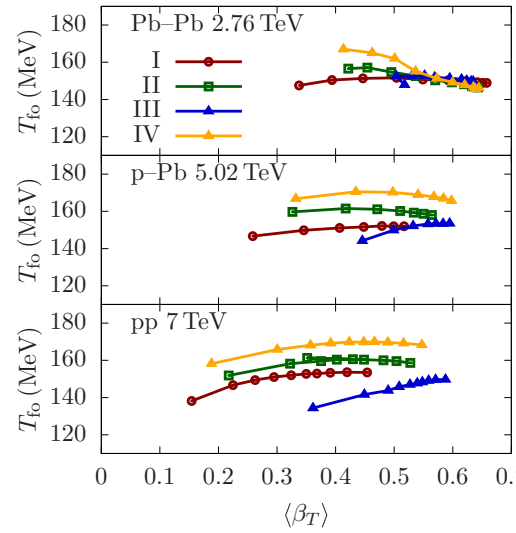

FIG. 6. Freeze-out temperature versus mean transverse flow for different p_T fit ranges (see Table VI) in a single freeze-out blast-wave model with resonance decays.

ACKNOWLEDGMENTS

A.M. thanks D. Devetak, A. Dubla, S. Floerchinger, E. Grossi, S. Masciocchi, I. Selyuzhenkov, and D. Teaney for the discussions and collaboration on related projects. The authors thank P. Parotto for sharing their PDG2016+ resonance and decay lists. The authors also thank A. Andronic, P. Braun-Munzinger, U. Heinz, P. Huovinen, W. Florkowski, A. Kalweit, J. Stachel, K. Reygers, and V. Vovchenko for useful discussions and comments. This work was supported in part by the German Research Foundation (Deutsche Forschungsgemeinschaft) Collaborative Research Centre "SFB 1225 (ISOQUANT)" (A.M.), the Danish Council for Independent Research–Natural Sciences, the Carlsberg Foundation, and the Danish National Research Foundation (DNRF) (V.V.). V.V. thanks the Institute for Theoretical Physics at Heidelberg University for the hospitality during a short term visit.

APPENDIX: BEST FIT PARAMETERS AND FIT RANGES

In Tables I–III we summarize the best fit values and uncertainties for different collision systems and centralities for single freeze-out blast-wave fits. In addition, in Tables IV and V we report the fit parameters for Pb-Pb collisions in different centrality bins within single freeze-out and partial chemical equilibrium models.

To study the model parameter sensitivity to different $p_{\rm T}$ regions, particle spectra are fitted in different transverse momentum intervals as summarized in Table VI. In addition to our nominal range (I), we consider the standard range (II), as well as high- and low-$p_{\rm T}$ regions (III, IV) used in previous publications by ALICE [15]. We find that for a given multiplicity, fit range (I) results in the lowest $\langle\beta_{\rm T}\rangle$ in all cases except for the most central Pb-Pb collisions as shown in Fig. 6. The freeze-out temperature measured in Pb-Pb

TABLE I. Results for π, K, p combined blast-wave fit with resonance decays for pp $\sqrt{s} = 7$ TeV data in momentum range $0.5 < p_T < 3.0$ (GeV/c).

Centrality	$\langle\beta_T\rangle$	$T_{\rm fo}$ (MeV)	n	dV/dy (fm^3)	χ^2/dof
0–1%	0.454 ± 0.004	154 ± 1	2.00 ± 0.04	57.7 ± 1.7	2.2
1–5%	0.420 ± 0.008	154 ± 1	2.32 ± 0.08	46.1 ± 1.3	3.1
5–10%	0.391 ± 0.008	153 ± 1	2.62 ± 0.09	39.3 ± 1.1	3.8
10–15%	0.368 ± 0.008	153 ± 1	2.91 ± 0.10	35.0 ± 1.0	4.4
15–20%	0.350 ± 0.008	153 ± 1	3.16 ± 0.11	31.7 ± 0.9	4.9
20–30%	0.324 ± 0.007	152 ± 1	3.56 ± 0.12	28.2 ± 0.8	5.7
30–40%	0.295 ± 0.007	151 ± 1	4.10 ± 0.15	24.2 ± 0.6	6.5
40–50%	0.263 ± 0.028	149 ± 1	4.85 ± 0.71	21.8 ± 0.3	7.6
50–70%	0.225 ± 0.007	147 ± 1	5.95 ± 0.25	18.7 ± 0.5	8.0
70–100%	0.154 ± 0.007	138 ± 1	9.43 ± 0.50	18.3 ± 0.6	8.2

TABLE II. Results for π, K, p combined blast-wave fit with resonance decays for p-Pb $\sqrt{s_{\rm NN}} = 5.02$ TeV data in momentum range $0.5 < p_T < 3.0\,({\rm GeV}/c)$.

Centrality	$\langle\beta_T\rangle$	$T_{\rm fo}$ (MeV)	n	dV/dy (fm^3)	χ^2/dof
0–5%	0.52 ± 0.01	152 ± 2	1.44 ± 0.05	122 ± 7	1.5
5–10%	0.50 ± 0.01	152 ± 1	1.57 ± 0.06	100 ± 3	2.0
10–20%	0.48 ± 0.01	152 ± 1	1.73 ± 0.05	85 ± 2	2.3
20–40%	0.45 ± 0.01	152 ± 1	2.00 ± 0.05	69 ± 2	3.1
40–60%	0.41 ± 0.01	151 ± 1	2.39 ± 0.09	51 ± 1	4.3
60–80%	0.35 ± 0.01	150 ± 1	3.19 ± 0.12	35 ± 1	5.8
80–100%	0.26 ± 0.01	147 ± 1	4.90 ± 0.20	19 ± 1	7.5

TABLE III. Results for π, K, p combined blast-wave fit with resonance decays for Pb-Pb $\sqrt{s_{\rm NN}} = 2.76$ TeV data in momentum range $0.5 < p_T < 3.0$ (GeV/c).

Centrality	$\langle\beta_T\rangle$	$T_{\rm fo}$ (MeV)	n	dV/dy (fm^3)	χ^2/dof
0–5%	0.66 ± 0.01	149 ± 1	0.34 ± 0.04	4273 ± 122	1.6
5–10%	0.65 ± 0.01	149 ± 1	0.39 ± 0.04	3585 ± 100	1.3
10–20%	0.64 ± 0.01	149 ± 1	0.44 ± 0.04	2682 ± 74	1.0
20–30%	0.62 ± 0.01	150 ± 1	0.55 ± 0.05	1796 ± 51	0.7
30–40%	0.59 ± 0.01	150 ± 1	0.71 ± 0.06	1188 ± 35	0.6
40–50%	0.55 ± 0.01	151 ± 1	0.96 ± 0.07	756 ± 23	0.5
50–60%	0.50 ± 0.01	152 ± 1	1.26 ± 0.09	428 ± 14	0.7
60–70%	0.45 ± 0.01	151 ± 1	1.74 ± 0.12	235 ± 9	1.2
70–80%	0.39 ± 0.02	150 ± 1	2.30 ± 0.17	117 ± 5	1.5
80–90%	0.34 ± 0.01	148 ± 1	3.08 ± 0.12	55 ± 2	2.9

TABLE IV. Results for π, K, p combined blast-wave fit with resonance decays for Pb-Pb $\sqrt{s_{\rm NN}} = 2.76$ TeV data in momentum range $0.5 < p_T < 3.0$ (GeV/c).

Centrality	$\langle\beta_T\rangle$	$T_{\rm fo}$ (MeV)	n	dV/dy (fm^3)	χ^2/dof
0–10%	0.65 ± 0.01	149 ± 1	0.36 ± 0.03	3925 ± 107	1.4
10–20%	0.64 ± 0.02	149 ± 1	0.44 ± 0.06	2682 ± 78	1.0
20–40%	0.61 ± 0.01	150 ± 1	0.61 ± 0.05	1489 ± 42	0.6
40–60%	0.53 ± 0.01	151 ± 1	1.07 ± 0.08	591 ± 19	0.6
60–80%	0.43 ± 0.02	151 ± 1	1.90 ± 0.14	175 ± 7	1.3

TABLE V. Results for π, K, p combined blast-wave fit with resonance decays in partial chemical equilibrium model with $T_{\rm chem} = 150$ MeV and $T_{\rm kin} = T_{\rm fo}$ for Pb-Pb $\sqrt{s_{\rm NN}} = 2.76$ TeV data in momentum range $0.5 < p_T < 3.0$ (GeV/c).

Centrality	$\langle\beta_T\rangle$	$T_{\rm fo}$ (MeV)	n	dV/dy (fm^3)	χ^2/dof
0–10%	0.65 ± 0.01	126 ± 2	0.57 ± 0.04	5990 ± 220	0.7
10–20%	0.64 ± 0.01	132 ± 2	0.59 ± 0.04	3710 ± 134	0.6
20–40%	0.61 ± 0.01	140 ± 3	0.69 ± 0.05	1810 ± 66	0.5
40–60%	0.53 ± 0.02	156 ± 3	1.04 ± 0.08	566 ± 23	0.6
60–80%	0.41 ± 0.02	184 ± 6	1.85 ± 0.17	106 ± 6	0.9

TABLE VI. Different choices of transverse momentum fit ranges (in GeV/c).

	π	K	p
I	[0.5,3.0]	[0.5, 3.0]	[0.5, 3.0]
II	[0.5,1.0]	[0.2, 1.5]	[0.2, 3.0]
III	[0.7,1.3]	[0.5, 1.5]	[1.0, 3.0]
IV	[0.5,0.8]	[0.2, 1.0]	[0.3, 1.5]

collisions shows little dependence on the fitting range, except at most peripheral bins. In smaller systems this dependence is more pronounced and shows a decreasing trend as higher transverse momenta are considered.

[1] A. Bazavov *et al.* (HotQCD Collaboration), Phys. Lett. B **795**, 15 (2019).
[2] A. Andronic, P. Braun-Munzinger, K. Redlich, and J. Stachel, Nature (London) **561**, 321 (2018).
[3] U. Heinz and R. Snellings, Annu. Rev. Nucl. Part. Sci. **63**, 123 (2013).
[4] D. A. Teaney, in *Quark-Gluon Plasma 4*, edited by R. C. Hwa and X.-N. Wang (World Scientific, Singapore, 2010), pp. 207–266.
[5] M. Luzum and H. Petersen, J. Phys. G **41**, 063102 (2014).
[6] C. Gale, S. Jeon, and B. Schenke, Int. J. Mod. Phys. A **28**, 1340011 (2013).
[7] R. Derradi de Souza, T. Koide, and T. Kodama, Prog. Part. Nucl. Phys. **86**, 35 (2016).
[8] J. E. Bernhard, J. S. Moreland, S. A. Bass, J. Liu, and U. Heinz, Phys. Rev. C **94**, 024907 (2016).
[9] E. Schnedermann, J. Sollfrank, and U. W. Heinz, Phys. Rev. C **48**, 2462 (1993).
[10] W. Broniowski and W. Florkowski, Phys. Rev. Lett. **87**, 272302 (2001).
[11] F. Retiere and M. A. Lisa, Phys. Rev. C **70**, 044907 (2004).
[12] S. Ryu, J.-F. Paquet, C. Shen, G. Denicol, B. Schenke, S. Jeon, and C. Gale, Phys. Rev. C **97**, 034910 (2018).
[13] S. A. Bass *et al.*, Prog. Part. Nucl. Phys. **41**, 255 (1998).
[14] H. Petersen, D. Oliinychenko, M. Mayer, J. Staudenmaier, and S. Ryu, Proceedings of the 27th International Conference on Ultrarelativistic Nucleus-Nucleus Collisions (Quark Matter 2018): Venice, Italy, May 14-19, 2018 [Nucl. Phys. A **982**, 399 (2019)].
[15] B. Abelev *et al.* (ALICE Collaboration), Phys. Rev. C **88**, 044910 (2013).
[16] B. I. Abelev *et al.* (STAR Collaboration), Phys. Rev. C **79**, 034909 (2009).
[17] S. Chatrchyan *et al.* (CMS Collaboration), Eur. Phys. J. C **74**, 2847 (2014).
[18] B. B. Abelev *et al.* (ALICE Collaboration), Phys. Lett. B **728**, 25 (2014).
[19] J. Adam *et al.* (ALICE Collaboration), Nat. Phys. **13**, 535 (2017).
[20] V. Begun, W. Florkowski, and M. Rybczynski, Phys. Rev. C **90**, 014906 (2014).
[21] I. Melo and B. Tomasik, J. Phys. G **43**, 015102 (2016).
[22] I. Melo and B. Tomášik, arXiv:1908.03023.
[23] G. Torrieri, S. Steinke, W. Broniowski, W. Florkowski, J. Letessier, and J. Rafelski, Comput. Phys. Commun. **167**, 229 (2005).
[24] N. S. Amelin, R. Lednicky, T. A. Pocheptsov, I. P. Lokhtin, L. V. Malinina, A. M. Snigirev, I. A. Karpenko, and Yu. M. Sinyukov, Phys. Rev. C **74**, 064901 (2006).
[25] B. Tomasik, Comput. Phys. Commun. **180**, 1642 (2009).
[26] M. Chojnacki, A. Kisiel, W. Florkowski, and W. Broniowski, Comput. Phys. Commun. **183**, 746 (2012).
[27] J. Sollfrank, P. Koch, and U. W. Heinz, Z. Phys. C **52**, 593 (1991).
[28] J. Sollfrank, P. Koch, and U. W. Heinz, Phys. Lett. B **252**, 256 (1990).
[29] M. Tanabashi *et al.* (Particle Data Group Collaboration), Phys. Rev. D **98**, 030001 (2018).
[30] A. Mazeliauskas, S. Floerchinger, E. Grossi, and D. Teaney, Eur. Phys. J. C **79**, 284 (2019).
[31] A. Mazeliauskas, S. Floerchinger, E. Grossi, and D. Teaney, FastReso–program for computing irreducible components of the particle distribution from direct resonance decays, GitHub repository, 2019, https://github.com/amazeliauskas/FastReso.
[32] F. Cooper and G. Frye, Phys. Rev. D **10**, 186 (1974).
[33] H. Bebie, P. Gerber, J. L. Goity, and H. Leutwyler, Nucl. Phys. B **378**, 95 (1992).
[34] T. Hirano and K. Tsuda, Phys. Rev. C **66**, 054905 (2002).
[35] P. Alba *et al.*, Phys. Rev. D **96**, 034517 (2017).
[36] P. Alba, V. Mantovani Sarti, J. Noronha, J. Noronha-Hostler, P. Parotto, I. Portillo Vazquez, and C. Ratti, Phys. Rev. C **98**, 034909 (2018).
[37] P. Parotto (private communication).
[38] C. Patrignani *et al.* (Particle Data Group Collaboration), Chin. Phys. C **40**, 100001 (2016).
[39] P. Huovinen, Eur. Phys. J. A **37**, 121 (2008).
[40] K. Aamodt *et al.* (ALICE Collaboration), J. Instrum. **3**, S08002 (2008).
[41] S. Acharya *et al.* (ALICE Collaboration), Phys. Rev. C **99**, 024906 (2019).
[42] J. Adam *et al.* (ALICE Collaboration), Phys. Lett. B **760**, 720 (2016).
[43] F. Becattini, M. Bleicher, E. Grossi, J. Steinheimer, and R. Stock, Phys. Rev. C **90**, 054907 (2014).
[44] V. Vovchenko, B. Dönigus, and H. Stoecker, Phys. Rev. C **100**, 054906 (2019).
[45] V. Vovchenko and H. Stoecker, Comput. Phys. Commun. **244**, 295 (2019).
[46] J. Adam *et al.* (ALICE Collaboration), Phys. Lett. B **758**, 389 (2016).
[47] B. B. Abelev *et al.* (ALICE Collaboration), Phys. Rev. Lett. **111**, 222301 (2013).
[48] B. B. Abelev *et al.* (ALICE Collaboration), Phys. Lett. B **728**, 216 (2014); **734**, 409(E) (2014).
[49] V. Vovchenko, K. Gallmeister, J. Schaffner-Bielich, and C. Greiner, Phys. Lett. B **800**, 135131 (2020).
[50] U. W. Heinz and J. S. Moreland, Proceedings of the 5th Biennial Workshop on Discovery Physics at the LHC (Kruger2018), J. Phys.: Conf. Ser. **1271**, 012018 (2019).
[51] K. Dusling, G. D. Moore, and D. Teaney, Phys. Rev. C **81**, 034907 (2010).
[52] D. Teaney and L. Yan, Phys. Rev. C **89**, 014901 (2014).
[53] P. Huovinen, P. F. Kolb, U. W. Heinz, P. V. Ruuskanen, and S. A. Voloshin, Phys. Lett. B **503**, 58 (2001).
[54] P. Braun-Munzinger, J. Stachel, and C. Wetterich, Phys. Lett. B **596**, 61 (2004).

[55] A. Ramamurti and E. Shuryak, arXiv:1811.03655.
[56] W. Florkowski, A. Kumar, R. Ryblewski, and A. Mazeliauskas, Phys. Rev. C **100**, 054907 (2019).
[57] A. Andronic, P. Braun-Munzinger, M. K. Köhler, K. Redlich, and J. Stachel, Phys. Lett. B **797**, 134836 (2019).
[58] R. Bellwied, J. Noronha-Hostler, P. Parotto, I. Portillo Vazquez, C. Ratti, and J. M. Stafford, Phys. Rev. C **99**, 034912 (2019).
[59] M. Bluhm and M. Nahrgang, Eur. Phys. J. C **79**, 155 (2019).
[60] A. Motornenko, V. Vovchenko, C. Greiner, and H. Stoecker, arXiv:1908.11730.
[61] D. Devetak, A. Dubla, S. Floerchinger, E. Grossi, S. Masciocchi, A. Mazeliauskas, and I. Selyuzhenkov, arXiv:1909.10485.